Molecular Therapy
Oncolytics
Original Article

SEC coupled with in-line multiple detectors for the characterization of an oncolytic Coxsackievirus

James Z. Deng,[1] Richard R. Rustandi,[1] Andrew Swartz,[2] Yvonne Shieh,[2] Jack B. Baker,[1] Josef Vlasak,[1] Shiyi Wang,[1] and John W. Loughney[1]

[1]Analytical Research & Development, Merck & Co., Kenilworth, NJ 07033, USA; [2]Process Research & Development, Merck & Co., Kenilworth, NJ 07033, USA

V937 is an oncolytic virus immunotherapy clinical drug candidate consisting of a proprietary formulation of Coxsackievirus A21 (CVA21). V937 specifically binds to and lyses cells with over-expressed ICAM-1 receptors in a range of tumor cell types and is currently in phase I and II clinical trials. Infectious V937 particles consist of a ~30 nm icosahedral capsid assembled from four structural viral proteins that encapsidate a viral RNA genome. Rapid and robust analytical methods to quantify and characterize CVA21 virus particles are important to support the process development, regulatory requirements, and validation of new manufacturing platforms. Herein, we describe a size-exclusion chromatography (SEC) method that was developed to characterize the V937 drug substance and process intermediates. Using a 4-in-1 combination of multi-detectors (UV, refractive index, dynamic and static light scattering), we demonstrate the use of SEC for the quantification of the virus particle count, the determination of virus size (molecular weight and hydrodynamic diameter), and the characterization of virus purity by assessing empty-to-full capsid ratios. Through a SEC analysis of stressed V937 samples, we propose CVA21 thermal degradation pathways that result in genome release and particle aggregation.

INTRODUCTION

In recent years, immunotherapies have been developed as powerful tools to fight many deadly and difficult to treat diseases. One promising approach utilizes oncolytic viruses to specifically target and destroy tumor cells and stimulate innate and adaptive immune responses.[1] V937 is an oncolytic virus immunotherapy clinical drug candidate that has been studied in a range of tumors that upregulate the cell-surface receptor ICAM-1 including melanoma, bladder cancer, and breast cancer. In early clinical trials, V937 demonstrated viral targeted tumor cell death with promising clinical outcomes and an acceptable safety profile.[2–5]

V937 consists of a proprietary formulation of Coxsackievirus A21 (CVA21), an enterovirus within the *Picornaviridae*. In mature *picornavirus* virions, single-stranded RNA (7.4 kb) is packed in an icosahedral capsid with 60 copies of VP1, VP2, VP3, and VP4 structural proteins.[6] The viral capsids assemble from protomer and pentamer subunits consisting of VP1, VP3, and the precursor protein VP0. Twelve pentamers can assemble into empty procapsids lacking a genome or encapsidate viral RNA to form provirions. The encapsidation of viral RNA triggers an autocatalytic cleavage of precursor VP0 to VP2+VP4 and the formation of mature virions (Figure 1).[7–9]

V937-infected cell culture harvests contain a distribution of empty and full CVA21 particles. Not all mature virions are infectious. However, genome-containing, mature virions with VP1, VP2, VP3, and VP4 are the only particles capable of oncolytic activity. Therefore, empty capsids and other non-infectious particles are considered a residual product impurity in the V937 drug substance (DS). The purification process was designed to remove particles with VP0 (empty procapsids, provirions) and enrich only genome-containing full capsids with VP2+VP4. The theoretical molecular weight (Mw) for a full capsid was calculated to be 8,203 kDa, based on known RNA and protein sequences.[10,11] The expected hydrodynamic diameter (Dh) is ~30 nm, based on structural and cryo-electron microscopy (cryo-EM) studies of other type A Coxsackieviruses.[12–16]

To characterize the V937 drug substance quality attributes and process the consistency, there remains a need for robust analytical tools that can detect total particles, particle size and aggregation, and empty/full particle ratios. To accomplish this, we developed a size-exclusion chromatography (SEC) method with 4-in-1 multi-detectors to characterize the V937 drug substance and to process intermediate samples. SEC, in combination with UV-(multi-angle light scattering-quasi-elastic light scattering)-refractive index (UV-(MALS-QELS)-RI) detectors, offers robust measurements of the virus particle concentration, the Mw, the hydrodynamic radius (Rh), and the empty/full capsid ratio.

Received 31 July 2021; accepted 9 December 2021;
https://doi.org/10.1016/j.omto.2021.12.009.

Correspondence: James Z. Deng, Analytical Research & Development, Merck & Co., Inc., Kenilworth, NJ 07033, USA.
E-mail: james_deng@merck.com

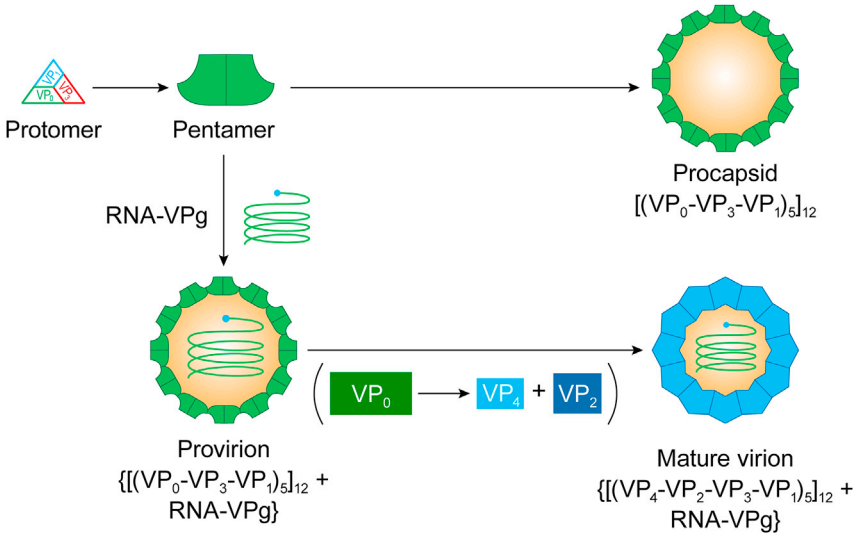

Figure 1. Assembly of picornavirus particles
Five protomers consisting of VP0-VP3-VP1 associate to form pentamers. Twelve pentamers may further assemble either into empty procapsids or may encapsidate the RNA genome to produce provirions. Mature virions are formed after VP0 cleavage into VP2+VP4.

RESULTS

SEC method development and virus peak identification

The SEC method was developed by screening various columns and an extensive optimization on pH, salt concentrations, and mobile phase modifiers (Table S2). Using the final SEC method described in the Materials and methods (SEC method and conditions) with UV, MALS-QELS, and RI detectors, the V937 drug substance exhibited a single Gaussian virus peak at 19.5 min in the SEC chromatography profile without observable aggregation or impurity peaks (Figure 2). Figure 2 illustrates the UV signal in red trace, MALS in black trace, QELS in cyan trace, and RI in blue trace. The UV and MALS signals are used to calculate the Mw through Zimm formalism and are plotted on the left side of the y axis. The Rh is calculated from dynamic light measured from a QELS detector and is plotted on the right side of the y axis. The V937 Rh of 14.8 nm, calculated from the measured translational diffusion coefficient through the Stokes-Einstein relationship by the SEC method, agrees with the reported *Picornavirus* Rh of 14–15 nm[7]. Furthermore, the measured Mw of 8,131 kDa on SEC is similar to the theoretical Mw of 8,203 kDa calculated from protein and RNA compositions of a full V937 capsid (Table S1B). These results are consistent with the sodium dodecyl sulphate–polyacrylamide gel electrophoresis (SDS-PAGE) analysis of the drug substance sample with no detectable VP0 (Figure 3), illustrating a negligible contribution from empty procapsids or provirions. The purity of our drug substance is also supported by cryo-EM images and SDS-PAGE for fractions collected from sucrose density gradient (Figures S5 and S6).

The SEC method can also determine the Rh and Mw for other intermediate process samples in various sample matrices and at different concentrations. V937 process intermediates exhibited similar SEC peak profiles and can be characterized without method modifications. The method can be easily employed to assist in future drug substance process development and to evaluate drug substance quality and consistency.

Analytical parameters

The multi-detector SEC assay measures the V937 particle count concentration and size in a drug substance. Therefore, standard analytical assay parameters were followed according to ICH2Q guidelines to evaluate the assay performance before qualification.

Specificity

The specificity was performed by a comparison of the chromatograms obtained from an injection of a sample to that which was obtained from a sample matrix (without V937). There was no peak observed from the sample matrix in the region of interest for the virus. The components in the sample matrix eluted after 25 min on the chromatogram, indicating the buffer analytes are much smaller than the virus and are well-separated from the virus peak (Figure S1).

Quantitation linearity

To evaluate the impact of V937 capsid particle loading on the SEC assay, the linearity of the assay was evaluated by injecting a sample from a 25 µL to 200 µL range. The particle number versus injection volume demonstrated an excellent linearity ($R^2 > 0.999$), as shown in Figure 4 (Table S3). This represents a linearity range from 7.1×10^{10} to 5.4×10^{11} particles for quantitation.

Repeatability and precision of quantitation

Repeatability for the particle concentration measurement of the assay was evaluated by injecting the sample five times on a single instrument. The calculated relative standard deviation (%RSD) of particle concentrations (particle/mL) from the experiment was used to assess intra-run precision. Three independent experiments were performed on different days using two different instruments/columns. The particle concentration intermediate precision was assessed from the overall %RSD value. Both intra-run precision and intermediate precision %RSD of the assay were <5% (Table S4).

Accuracy of quantitation

An analysis of SDS-PAGE (Figure 3) suggests that the V937 drug substance contains only mature virions with no VP0. Because each full particle is expected to contain only one genome, the drug substance virus particle concentration should be equal to the concentration of genome copies. The SEC quantitation accuracy was evaluated by comparing the capsid particle concentration

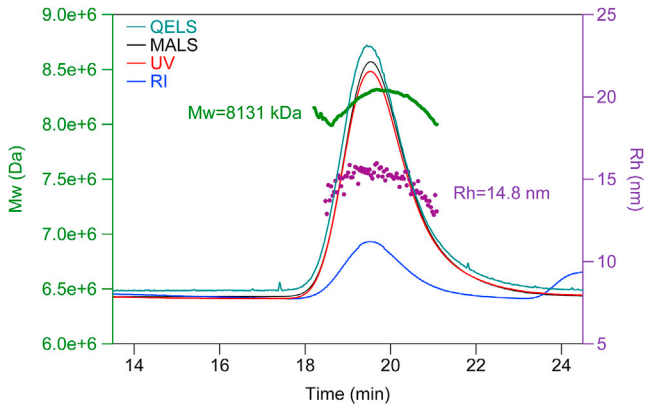

Figure 2. SEC chromatograms of V937 DS with size and Mw distribution

The left y axis describes the Mw (Da) detected by MALS, and the right y axis represents hydrodynamic radius (Rh [nm]) measured by QELS. The red trace is the UV signal at A280 nm, the black trace is the MALS signal, the cyan trace is QELS, and the blue trace is the RI signal. DS was detected as a peak at ~19 min, and sample matrix components elute after 24 min. The green line across the peak represents the particle Mw distribution, while the dotted purple line represents the particle Rh distribution.

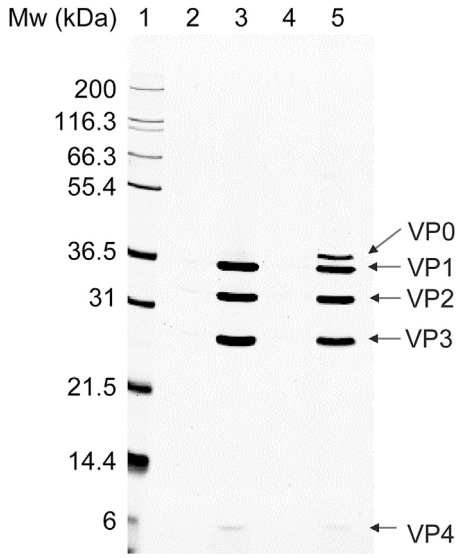

Figure 3. Analysis of viral proteins by SDS-PAGE

Viral proteins VP0, VP1, VP2, VP3, and VP4 are indicated in process intermediate samples. VP0 is not detectable in DS. Lane 1: Mw marker; lane 2: blank; lane 3: V937 DS; lane 4: blank; lane 5: process intermediate.

(particles/mL) with the genome copy concentration (copies/mL), as detected by a quantitative reverse transcription PCR (qRT-PCR) assay. This orthogonal method was used because a virus standard for a spike experiment was not available. Four drug substance batches were analyzed by both assays, and the percentage of accuracy was determined by the ratio of particle-to-genome concentrations. The results ranged from 84% to 92% (Table 1), indicating that the SEC assay has a comparable accuracy to the well-established qRT-PCR technique.

Virus recovery

Virus recovery from the SEC method was evaluated by comparing the virus concentrations obtained from SEC chromatography with those from direct UV A280 measurement on a UV-visible (Vis) spectrometer. The reported A280 spectrometer measurement represented an average result from two measurements for each sample, and similarly duplicate injections were averaged for the SEC method. The UV method is a bulk-sample measurement that detects all absorbing species in the sample. We expect this bulk measurement to align with the SEC data because the drug substance sample is highly purified and only one peak is observed during the SEC experiments. The SEC method achieved an average 99% recovery for the four batches measured (Table 2). This represents an acceptable recovery of viral particles off the column to ensure the calculated virus concentration does not have any biases due to column interactions.

Batch-to-batch consistency

The optimized SEC method was used to evaluate the V937 process consistency by analyzing four different drug substance batches (Table 3). The Mw and Rh calculated from the SEC virus peak represent the expected characteristics of the Coxsackievirus and demonstrated good batch-to-batch process consistency.

Characterization of empty and full capsid particles in mixed virus samples

The empty/full ratio is considered to be a key product quality attribute that has implications on drug substance quality. Characterization of the empty/full ratio is a focus of increased research in the virus and gene delivery fields.[17,18] An array of analytical methods, such as analytical ultracentrifugation (AUC), ion-exchange high-performance liquid chromatography (IEX HPLC), and cryo-EM, have been developed or are under development for this purpose.

Two sample sets containing high empty procapsid content were compared to the V937 drug substance to evaluate the SEC method's ability to quantitate both full and empty virus particles and the empty/full ratio. The first sample was purified empty procapsids isolated from the chromatography step that removed empty capsids from the V937 drug substance process described in the materials and methods (V937 drug substance production). The second sample was a mixture of full and empty V937 capsids that were purified from a cell culture harvest by omitting the step that cleared empty capsids in the drug substance process described in the materials and methods (V937 drug substance production). The measured particle sizes (Rh ~15 nm) were distributed uniformly across the peaks for drug substance (full), empty viruses, and the empty/full mixture as their size is not expected to change, as shown in Figure 5A. The measured Mws were 8,200, 5,828, and 7,195 kDa for full, empty, and empty/full mix samples, respectively (Figure 5B). The experimentally measured Mw of full and empty particles agrees well

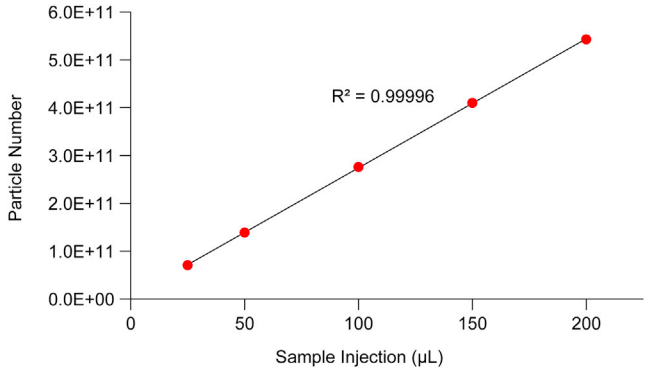

Figure 4. Particle number linearity curve

The particle number in DS versus the injection volume demonstrates a linear relationship with $R^2 > 0.9999$.

with the expected theoretical Mw of 8,203 and 5,821 kDa, respectively.

To quantify the empty/full ratio of the mixed virus samples, the Wyatt Astra protein conjugate method described in the materials and methods (SEC method and conditions) was applied to deconvolute the virus peak. The cleavage of VP0 in an empty procapsid to VP2 and VP4 after genome encapsidation does not change the virus protein content (VP0 = VP2 + VP4). Therefore, empty procapsids and mature virions are expected to have equal amounts of protein in each capsid, and viral RNA is utilized as a modifier for the protein in the analysis. The full virus particle concentration (particle/mL) was calculated from the measured RNA concentration as in Equation 2 using the RNA Mw (2,382 kDa), and the total particle concentration (particle/mL) was calculated from the measured total protein concentration using Equation 2 with the capsid protein Mw (5,821 kDa).

The mixed sample has an average Mw of 7,195 kDa, which represents both full and empty particles (i.e., total particles). Consequently, the empty particle concentration was calculated by subtracting the full particles from total particles. The calculations are described in the materials and methods (SEC method and conditions) and detailed in the supplemental information. The calculated empty/full ratio for this empty/full mixture virus sample was 0.81, indicating that about 45% of the total particles were empty particles (Table S5). The empty/full ratio is a critical attribute that represents viral purity and can be used to track empty capsid clearance in process and process consistency. This method has been demonstrated to be useful for measuring the empty/full ratio, but its sensitivity remains under evaluation.

Study of the stressed V937 samples and the thermal degradation pathway

To determine if the optimized SEC method can be used to monitor particle degradation, V937 drug substance samples were studied under elevated temperatures (37°C, 45°C, and 60°C) and held across multiple days prior to the SEC analysis for each time point. Control V937 samples at 4°C and 22°C are not prone to thermal degradation under experimental conditions. Data summarized in Table 4 and Figure 6A show that no V937 particle degradation was detected when stored at 37°C for up to 7 days, with only minor changes in particle size (Rh) and Mw observed after 7 days at 37°C.

Table 1. Accuracy by comparison with a qRT-PCR assay

Samples	[genome copy] (copies/mL) (GQA)	[virus particle] (particles/mL) (SEC)	SEC/GQA (%)
Batch 1	3.12×10^{12}	2.79×10^{12}	89
Batch 2	1.91×10^{12}	1.61×10^{12}	84
Batch 3	1.46×10^{12}	1.34×10^{12}	92
Batch 4	1.76×10^{12}	1.60×10^{12}	91
Average			87
%RSD			4.1

When the stressed temperature was elevated to 45°C for 2 h, a much broader virus peak with several shoulders appeared. The detected species in this peak have higher polydispersity but maintain a UV A260/280 ratio from 1.6 to 2.0 (Figure S2). This suggests that at short timescales at 45°C, viral capsid proteins may begin to partially unfold, but the RNA remains encapsidated or particle-associated. After 48 h at 45°C, one species with a lower Mw of 5,802 kDa and a reduced A260/A280 ratio of <1.0 was observed. The Mw matches the calculated Mw for an empty viral particle, and the A260/A280 ratio is indicative of a particle without absorbance contributions from RNA. A smaller species with an A260/A280 value of ~2 was observed at retention time just before column inclusion volume (Figure S3). These data indicate a time-dependent degradation mechanism at 45°C where full viral capsids initially unfold then release the viral RNA, resulting in empty virus particles with the same particle size (unchanged Rh).

When stress-testing was carried out at 60°C, within the first hour, higher-Mw species with two distinct particle sizes were detected, consisting of the original peak (Rh = 13 nm) or a significantly enlarged species (Rh = 70 nm). The larger species that eluted at room temperature (RT) after ~15 min had a Mw of 390 MDa, while the later elution peak was polydisperse with a Mw of 16.7 MDa (Figure 6A, red trace). These results suggest that virus disintegration and aggregation occurred at 60°C, which agrees with the reported melting point of ~65°C from reported Coxsackievirus.[13] A260/A280 ranging from 1.5 to 1.9 for both species suggests that genetic RNA materials may remain embedded or attached to these aggregated particles. After 24 h at 60°C, the virus aggregate peak became undetectable. Instead, aggregated protein species and degraded RNA species could be observed (Figure S4).

V937 thermal aggregation was further evaluated by dynamic light scattering (DLS). The particle size and light scattering intensity were monitored across a temperature gradient from 25°C to 65°C.

Table 2. Evaluation of SEC method recovery

Method	UV spectra measurement (n = 2)		SEC measurement (n = 2)	Recovery
DS sample batch	A_{280}(avg)	[virus] (μg/mL)	[virus] (μg/mL)	SEC/UV (%)
Batch 1	0.197	35.9	37.0	103
Batch 2	0.119	21.7	21.3	98
Batch 3	0.122	22.3	18.7	84
Batch 4	0.108	19.6	21.5	110
Average				99

Table 3. Batch-to-batch comparison of V937

V937 DS batch	Mw (kDa)	DPI (Mw/Mn)	Rh (nm)
Batch 1	8546	1.02	16.2
Batch 2	8122	1.00	14.8
Batch 3	8184	1.01	14.5
Batch 4	8073	1.01	14.6
Average	8231	1.01	15.0
%RSD	3.2	0.4	1.4

The data shown in Figure 6B demonstrate that the particle size and light scattering intensity remained constant until a significant aggregation was detected in a transition region between 52°C and 60°C, which agrees with SEC results. Furthermore, the measured particle size (Rh ∼16 nm) by DLS agreed well with SEC, and interestingly, the observed Rh ∼70 nm at 60°C within the first hour in SEC was also observed in DLS at ∼54°C.

Based on these observations, we propose two V937 thermal degradation pathways: virus aggregation and RNA escape (Figure 7).[19,20] Both pathways could lead to aggregated virion proteins and degraded RNAs over time. These two degradation pathways could coexist in parallel or happen sequentially, depending on the sample environment (temperature, pH, osmolality). Using this method to understand the virus property and stability at various stages would assist in future process investigations and troubleshooting and in assessing the impact of process change. Forced degradation studies can be performed at these elevated temperature conditions to satisfy regulatory requirements.

DISCUSSION

Although Coxsackieviruses have been characterized by structural tools, such as X-ray and cryo-EM, there are no previous reports for a chromatography method. Here, we have developed a SEC-UV-(MALS-QELS)-RI method to analyze our oncolytic Coxsackievirus clinical candidate, V937. We demonstrated that SEC could separate and characterize multiple attributes for an assembled single virion in a single run. The virus particle size and Mw can be determined from light scattering signals with good accuracy and consistency. Virus particle concentrations can be quantified from a UV detector with good accuracy, precision, and linearity. We expanded the application of the Wyatt Astra protein conjugation method to analyze viruses containing protein and nucleic acid components. Mixed viruses containing both empty and full capsids can be characterized and quantified by employing this protein conjugate method. The virus concentrations (particle/mL) for both empty and full viral particles and the empty/full ratio can be deduced from this analysis. We have also demonstrated that this assay can be used to monitor virus thermal stability and the proposed potential degradation mechanism. The V937 drug substance exhibited a consistent Mw and particle size distribution from batch to batch. The method presented in this paper can have broader applications toward other types of non-enveloped and small-enveloped vaccines and viral vectors.

MATERIALS AND METHODS

Reagents and materials

Bis-Tris-HCl 1M solution was purchased from Rigaku Reagents (Seattle, WA, USA). Sodium chloride 5M solution was bought from Promega (Madison, WI, USA). BSA Standard Ampules (2 mg/mL), Novex WedgeWell 16%, Tris-Glycine, 1.0 mm, Mini Protein Gel, Mark12 Unstained Mw marker, and SYPRO Ruby Protein Gel Stain Solution were all purchased from ThermoFisher (Waltham, MA, USA). The PCR primers and TaqMan probe were purchased from Applied Biosystems (Foster City, CA, USA). The synthetic RNA oligonucleotide was purchased from Integrated DNA Technologies (Coralville, IA, USA).

V937 drug substance production

Briefly, the V937 drug substance was produced from infected MRC-5 cells (derived from ECACC 05072101) cultured in a microcarrier bioreactor using a virus seed derived from a CVA21 Kuykendall prototype strain (ATCC VR-850). Lysates were harvested and clarified through depth filters to remove cell debris. The clarified harvest was purified across an affinity chromatography and two polishing IEX chromatography steps to concentrate and clear residual impurities and procapsids. Purified V937 was exchanged into a stabilizing buffer and passed through a 0.2 μm filter to generate the final drug substance.

SDS-PAGE analysis of V937 viral proteins

To characterize the viral protein content in V937 process intermediates and drug substance, samples were analyzed by SDS-PAGE under reducing conditions. Briefly, 75 μL of each sample was mixed with a 25 μL 4X reducing sample buffer containing the reducing agents DTT and SDS and denatured on a heat plate at 70°C for 10 min. SDS-PAGE gel was performed using Novex WedgeWell 16%, Tris-Glycine, 1.0 mm, and Mini Protein Gel with a runtime of 90 min at 150 V at ambient temperature. The sample volume loaded into the gel was 40 μL. The protein bands were visualized by SYPRO Ruby Protein Gel Stain at ambient temperature. The image was acquired using the Gel Doc EZ Imager from Bio-Rad (Hercules, CA, USA).[21]

Measurement of V937 drug substance UV absorbance

The V937 drug substance was measured by UV using a Cary 3500 UV-Vis spectrophotometer from Agilent (Wilmington, DE,

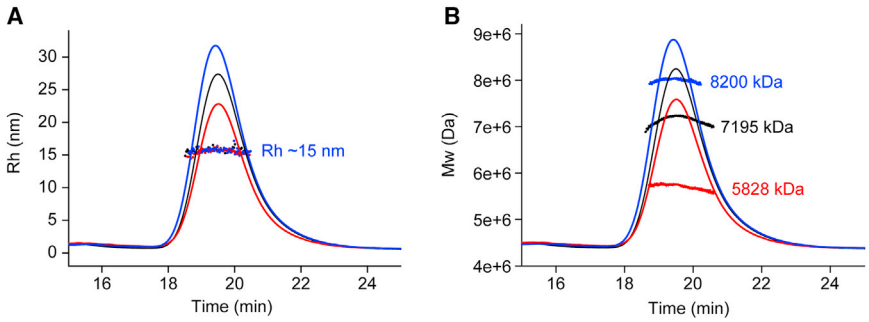

Figure 5. Comparison of Rh and Mw for empty, full, and empty/full mixture viral capsids

LS signals are normalized by concentration factors. All samples eluted out at the same retention time on the chromatogram. The blue trace represents full virus, the black trace represents empty/full mixture, and the red trace is empty virus. (A) All three virus samples (empty, full, and empty/full mix) have indistinguishable Rh values (~15 nm), represented by the dotted lines across the peak. (B) The measured Mw from these three samples are different, with 8,200 kDa for full virus (blue line across the peak), 7,195 kDa for empty/full mixture (black line across the peak), and 5,828 kDa for empty virus (red line across the peak).

USA). Samples were pipetted into a 1 cm Quartz UV cuvette (Hellma Analytics, High Precision Cell), and the absorbance at 280 nm (A280) was measured. The signal was buffer-subtracted using the V937 stabilizing buffer in the reference channel, and the concentration was calculated using a V937 extinction coefficient of 5.48 mL/(mg×cm) (see Table S1B). Each sample was measured in duplicate, and the average of the two measurements is reported.

qRT-PCR assay for genome quantitation

Viral genomes were measured by 1-step qRT-PCR. The V937 drug substance was lysed using proteinase K and SDS at 37°C for 30 min, followed by a nucleic acid extraction.[22] Briefly, the sample lysate was mixed with phenol:chloroform:isoamyl alcohol, followed by phase separation. Nucleic acids were precipitated from the aqueous phase using sodium acetate and isopropanol, pelleted, then washed with ethanol. Nucleic acid pellets were dried in an oven at 37°C then resuspended in nuclease-free water overnight.

The qRT-PCR assay uses a TaqMan dual-labeled probe, designed against GenBank: AF465515.1, and targets a 101-nucleotide sequence in the CVA21 VP1 gene. The genome copy number was determined by interpolation against a standard curve of a synthetic RNA (Integrated DNA Technologies, Coralville, IA, USA) containing the VP1 gene target region, ranging from 1×10^{11} to 1×10^{7} genome copies/mL. Nucleic acids extracted from samples were diluted in nuclease-free water prior to qRT-PCR to avoid extrapolation, as needed. All qRT-PCRs were performed on ABI 7900HT, ViiA 7, or QuantStudio 5 instruments (Applied Biosystems, Foster City, CA, USA). Each sample was measured in triplicate wells, and the average of the triplicate measurements is reported.

Table 4. Stability of stressed virus

Peaks		Main virus peak (RT ~19 min)			
Temp (°C)	Incubation time	Mw (kDa)	PDI (Mw/Mn)	Rh (nm)	A_{260}/A_{280}
37	2 h	8271	1.01	13.1	1.7
	24 h	8545	1.00	13.4	1.7
	7 days	7819	1.01	15.8	1.7
45	2 h	9602	1.24	10.1	1.8
	2 days	5802	1.01	13.0	0.9
60	1 h	16,672	1.55	13.9	1.9
	24 h	27,233	1.08	12.6	0.5

DLS temperature trend measurement

DLS was performed using a Zetasizer ZSP instrument (Malvern Analytical, Malvern, UK) with a 10 mW laser at 633 nm and a 173° scattering angle. A purified V937 sample was dispensed into a low-volume cuvette (ZEN0040, Malvern), and the scattering intensity was measured in triplicate at 1°C intervals across a temperature ramp from 25°C to 65°C with a 30 s equilibration time between measurements. The data were analyzed by the Protein Analysis algorithm provided by the Malvern Zetasizer software using a sample RI of 1.45, an absorption of 0.001, and a dispersant RI of 1.33.

SEC method and conditions

The liquid chromatography separation was performed on an Agilent 1260 Infinity II Bioinert system (Agilent, Wilmington, DE, USA) equipped with an integrated degassing unit, a quaternary pump, an autosampler, and a UV−Vis diode array detector. A TSKgel-G5000PW column (7.8 mm × 30 cm, 13 µm particle size, Tosoh Bioscience, Tokyo, Japan) was used for the separation condition with a 10 mM Bis-Tris, 600 mM NaCl, and pH 6.9 mobile phase. An optimized flow rate of 0.4 mL/min was employed to avoid high system pressure. Column temperature was set at 30°C, and the HPLC runtime was 35 min for each injection.

Several in-line detectors including a MALS detector (DAWN or Mini-DAWN) and an Optilab T-rEX RI detector (Wyatt Technology, Santa Barbara, CA, USA) were connected in series to the UV-Vis diode array detector. A DLS detector (WyattQELS QELS module) is embedded in the MALS detector and positioned at a 135° scattering angle. The WyattQELS module and MALS detector collect DLS and multi-angle static light scattering signals from the sample, respectively and simultaneously. The detectors were connected in the following order: SEC-UV-(MALS-QELS)-RI. The light scattering detector (MALS) was calibrated using toluene, and the detectors were normalized using a BSA standard according to the manufacturer's instructions. The original retention times of the signal from different detectors are different due to the

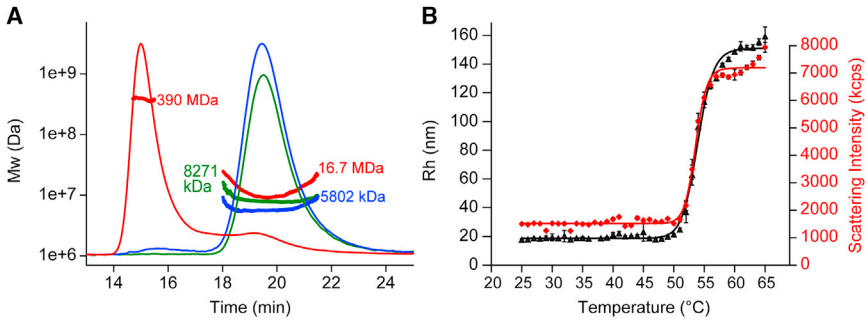

Figure 6. Analysis of V937 DS thermal stability by SEC-UV-(MALS-QELS)-RI and DLS

(A) Comparison of samples Stressed at 37°C, 45°C and 60°C on SEC-UV-MALS(QELS)-RI. Red trace is for sample stressed at 60°C, blue is for 45°C stressed sample and green trace is for sample at 37°C. Mw for each species is shown by the lines across the peaks. (B) DLS Temperature Study. Rh (black) and scattering intensity (red) were measured across a temperature gradient from 25 to 65°C in triplicate. A size and scattering increase was observed between 50°C and 60°C.

sequential connections. Peak alignment and band broadening were performed with a monodisperse BSA standard, and the aligned chromatographic data are reported. All data were collected and analyzed with ASTRA 7 software. A first-order fit Zimm formalism is used for all Mw calculations. The Rh is calculated from the measured translational diffusion coefficient through the Stokes-Einstein relationship.[23,24]

The UV A280 extinction coefficients for both empty and full virus particles were calculated from known CVA21 virion protein (VP) and RNA sequences using tools and equations in the references.[10,11,25–27] The calculated UV A280 extinction coefficient for a full CVA21 virus is 5.48 mL/(mg●cm) and for an empty virus is 1.33 mL/(mg●cm) (Tables S1A and S1B).

Because no detectable VP0 in the V937 drug substance was observed by SDS-PAGE (Figure 3), the drug substance samples were assumed to consist of only full virus particles. The mass of these samples was calculated from a virus A280 nm peak on the SEC using Wyatt Astra 7 software (UV A280 as the concentration source). The virus concentration was calculated from virus mass in Equation 1.

$$\textbf{Virus Concentration}\ (\mu\textbf{g}/\textbf{mL}) = \left(\frac{\textbf{Virus mass}\ (\mu\textbf{g})}{\textit{Injection Volume}\ (\textit{mL})}\right) \quad \text{(Equation 1)}$$

The virus particle concentration was obtained by Equation 2 using an Avogadro constant and the theoretical Mw of a full virus particle. The contribution from empty procapsids was assumed to be negligible because of the high full particle purity of the drug substance determined by SDS-PAGE.

$$\textit{Particle Concentration}\left(\frac{\textit{particle}}{\textit{mL}}\right) = \left(\frac{\textbf{Virus Concentration}\ (\textbf{g}/\textbf{mL})}{\textit{Mw}\ (\textit{Da})}\right) * \textit{N} \quad \text{(Equation 2)}$$

Note that N: Avogadro constant (6.02×10^{23} mol^{-1}).

Empty and full Coxsackievirus viral particles are indistinguishable by size.[13] A single virus peak was observed in the SEC chromatogram when injecting a mixture of empty and full capsids. An analysis of the virus mixture was performed using the Wyatt protein conjugate method on the peak.[28,29] The basis of this analysis is derived from the unique combinations of signals from three detection channels: UV (A280), differential RI, and static light scattering (LS). Protein and RNA contents in virus particles were considered as two separate, measurable attributes (protein and modifier) and deconvoluted in the protein conjugate analysis based on their unique UV extinction coefficients and RI increment (dn/dc) values. The protein conjugate analysis method calculates the molar mass of each component in the conjugate as well as the mass fraction of the two components. Beer Lambert Law was applied to measure the concentration from the UV channel, and the measured concentration can be converted to molar mass. The RI increment (dn/dc)

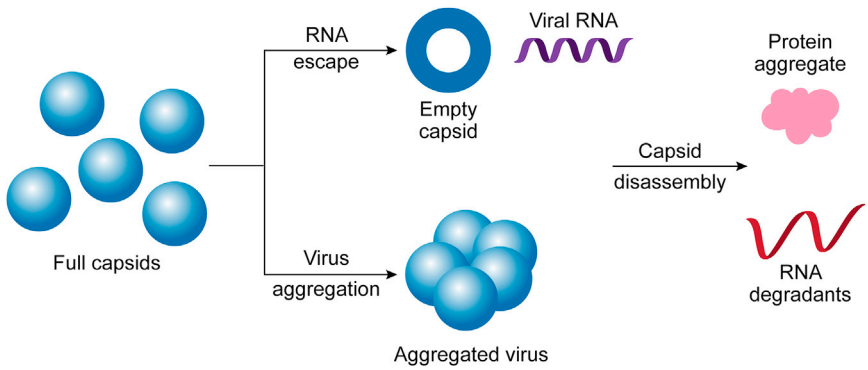

Figure 7. Proposed V937 thermal degradation pathways

Mature virions may degrade under thermal stress through RNA escape or/and virus aggregation pathways. At extended exposure to elevated temperatures, the empty capsids and capsid aggregates may further unfold into disassembled subunits that aggregate and/or degrade.

was used similarly to calculate the concentration from RI channel C_{dRI}, as in Equation 3.

$$CdRI = \frac{\Delta n}{(dn/dc)} \quad \text{(Equation 3)}$$

Note that Δn is the change in RI as measured by the RI detector.

The generic protein dn/dc value of 0.185 mL/g and the nucleic acid dn/dc value of 0.170 mL/g for RNA were applied. Both dn/dc values were based on reported literature values[30–32] and calibrated to the LS laser wavelength used in the author's lab and which was provided to the authors courtesy of Wyatt Technology. In the analysis, the virus protein content (for both empty and full) was calculated and reported as protein mass, while the RNA content was reported as the modifier mass. The RNA mass was converted to the particle number for full virions (RNA number) following Equations 1 and 2 using Mw of the virus RNA only. The total particle number (empty + full viruses) was calculated in the same fashion using protein mass and the Mw of an empty virus (protein only). The calculation parameters are listed below (from Tables S1A and S1B).

Virus content	Mw (kDa)	Dn/dc (mL/g)	A280 Coeff ($mL*mg^{-1}\ cm^{-1}$)
Virus proteins	5821	0.185	1.33
Virus RNA	2382	0.170	15.6

Data availability statement

The datasets generated and/or analyzed during the current study are available from the corresponding author on reasonable request.

SUPPLEMENTAL INFORMATION

Supplemental information can be found online at https://doi.org/10.1016/j.omto.2021.12.009.

ACKNOWLEDGMENTS

This work was fully funded by Merck Sharp & Dohme Corp., a subsidiary of Merck & Co., Inc., Kenilworth, NJ, USA. We also would like to extend our gratitude to our Merck & Co., Kenilworth, NJ, USA Vaccine Upstream and Downstream Process Development Teams colleagues for providing us with purified V937 materials. We would like to thank Wyatt Technology (Santa Barbara, CA, USA) for providing dn/dc values to the authors.

AUTHOR CONTRIBUTIONS

Conceptualization, J.Z.D., R.R.R., A.S.; methodology, J.Z.D., A.S., R.R.R.; investigation, J.Z.D., J.B.B., Y.S., S.W., J.V.; writing – original draft, J.Z.D.; writing – review & editing, R.R.R., A.S., J.W.L.; supervision and project administration, R.R.R., J.W.L.

DECLARATION OF INTERESTS

The authors declare no competing interests

REFERENCES

1. Lemos de Matos, A., Franco, L.S., and McFadden, G. (2020). Oncolytic viruses and the immune system: the dynamic duo. Mol. Ther. Methods Clin. Dev. *17*, 349–358.
2. McCarthy, C., Jayawardena, N., Burga, L.N., and Bostina, M. (2019). Developing picornaviruses for cancer Therapy. Cancers *11*, 685.
3. Bradley, S., Jakes, A.D., Harrington, K., Pandha, H., Melcher, A., and Errington-Mais, F. (2014). Applications of coxsackievirus A21 in oncology. Oncolytic Virother. *3*, 47–55.
4. Annels, N.E., Arif, M., Guy, R., Simpson, G.R., Denyer, M., Moller-Levet, C., Mansfield, D., Butler, R., Shafren, D., Au, G., et al. (2018). Oncolytic immunotherapy for bladder cancer using coxsackie A21 virus. Mol. Ther. Oncolytics *9*, 1–12.
5. Annels, N.E., Mansfield, D., Arif, M., Ballesteros-Merino, C., Simpson, G.R., Denyer, M., Sandhu, S.S., Melcher, A.A., Harrington, K.J., Davies, B., et al. (2019). Phase I trial of an ICAM-1-targeted immunotherapeutic-coxsackievirus A21 (CVA21) as an oncolytic agent against non muscle-invasive bladder cancer. Clin. Cancer Res. *25*, 5818–5831.
6. Chuan, X., Bator-Kelly, C.M., Rieder, E., Chipman, P.R., Craig, A., Kuhn, R.J., Wimmer, E., and Rossmann, M.G. (2005). The crystal structure of coxsackievirus A21 and its interaction with ICAM-1. Structure *13*, 1019–1033.
7. Tuthill, T.J., Groppelli, E., Hogle, J.M., and Rowlands, D.J. (2010). Picornaviruses. Curr. Top. Microbiol. Immunol. *343*, 43–89.
8. RacanielloPicornaviridae V.R. The Viruses and Their Replication. Fields Virology. Fifth Edition Lippincott Williams & Wilkins. p. 795-838.
9. Jiang, P., Liu, Y., Ma, H.C., Paul, A.V., and Wimmer, E. (2014). Picornavirus morphogenesis. Microbiol. Mol. Biol. Rev. *78*, 418–437.
10. Hughes, P.J., North, C., Minor, P.D., and Stanway, G. (1989). The complete nucleotide sequence of coxsackievirus A21. J. Gen. Virol. *70*, 2943–2952.
11. Newcombe, N.G., Andersson, P., Johansson, E.S., Au, G.G., Lindberg, A.M., Barry, R.D., and Shafren, D.R. (2003). Cellular receptor interactions of C-cluster human group A Coxsackieviruses. J. Gen. Virol. *84*, 3041–3050.
12. Shen, C., Liu, Q., Zhou, Y., Ku, Z., Wang, L., Lan, K., Ye, X., and Huang, Z. (2016). Inactivated coxsackievirus A10 experimental vaccines protect mice against lethal viral challenge. Vaccine *34*, 5005.
13. Zhu, L., Sun, Y., Fan, J., Zhu, B., Cao, L., Gao, Q., Zhang, Y., Liu, H., Rao, Z., and Wang, X. (2018). Structures of coxsackievirus A10 unveil the molecular mechanisms of receptor binding and viral uncoating. Nat. Commun. *9*, 4985.
14. Xu, L., Zheng, Q., Li, S., He, M., Wu, Y., Li, Y., Zhu, R., Yu, H., Hong, Q., Jiang, J., et al. (2017). Atomic structures of coxsackievirus A6 and its complex with a neutralizing antibody. Nat. Commun. *8*, 505.
15. Chen, J., Ye, X., Zhang, X.Y., Zhu, Z., Zhang, X., Xu, Z., Ding, Z., Zou, G., Liu, Q., Kong, L., et al. (2019). Coxsackievirus A10 atomic structure facilitating the discovery of a broadspectrum inhibitor against human enteroviruses. Cell Discov. *5*, 4.
16. Liu, C.C., Guo, M.S., Wu, S.R., Lin, H.Y., Yang, Y.T., Liu, W.C., Chow, Y.H., Shieh, D.B., Wang, J.R., and Chong, P. (2016). Immunological and biochemical characterizations of coxsackievirus A6 and A10 viral particles. Antivir. Res. *129*, 58–66.
17. Fu, X., Chen, W., Argento, C., Clarner, P., Bhatt, V., Dickerson, R., Bou-Assaf, G., Bakhshayeshi, M., Lu, X., Bergelson, S., et al. (2019). Analytical strategies for quantification of adeno-associated virus empty capsids to support process development. Hum. Gene Ther. Methods *30*, 144–152.
18. Hajba, L., and Guttman, A. (2020). Recent advances in the analysis full/empty capsid ratio and genome integrity of adeno-associated virus (AAV) gene delivery vectors. Curr. Mol. Med. *20*, 806–813.
19. Buchta, D., Füzik, T., Hrebík, D., Levdansky, Y., Sukeník, L., Mukhamedova, L., Moravcová, J., Vácha, R., and Plevka, P. (2019). Enterovirus particles expel capsid pentamers to enable genome release. Nat. Commun. *10*, 1138.
20. Bostina, M., Levy, H., Filman, D.J., and Hogle, J.M. (2011). Poliovirus RNA is released from the capsid near a twofold symmetry Axis. J. Virol. *85*, 776–783.
21. David, E.G. (1990). Method Enzymol. *182*, 425–441.

22. Moore, D., and Dowhan, D. (2002). Purification and concentration of DNA from aqueous solutions. Curr. Protoc. Mol. Biol. *59*, 2.1.1–2.1.10.22.

23. Huglin, M.B. (1972). Light Scattering from Polymer Solutions Chapter 5 (Academic Press).

24. Wyatt, P.J. (1993). Light scattering and the absolute characterization of macromolecules. Anal. Chim. Acta *272*, 1–40.

25. Gasteiger, E., Hoogland, C., Gattiker, A., Duvaud, S., Wilkins, M.R., Appel, R.D., and Bairoch, A. (2005). Protein Identification and Analysis. *The Proteomics Protocols Handbook* (Humana Press. Tool on the ExPASy Server), https://web.expasy.org/protparam.

26. Murugaiah, V. (2011). Determination of Extinction Coefficient. Handbook of Analysis of Oligonucleotides and Related Products (CRC Press), Tool: "Quest Calculate™ RNA Molecular Weight Calculator." AAT Bioquest, Inc,, https://www.aatbio.com/tools/calculate-RNA-molecular-weight-mw.

27. Sambrook, J., and Russell, D.W. (2001). Extraction, Purification, and Analysis of mRNA from Eukaryotic Cells. *Molecular Cloning - A LABORATORY MANUAL* Chapter 7 (COLD SPRING HARBOR LABORATORY PRESS).

28. Kendrick, B.S., Kerwin, B.A., Chang, B.S., and Philo, J.S. (2001). Online size-exclusion high-performance liquid chromatography light scattering and differential refractometry methods to determine degree of polymer conjugation to proteins and protein-protein or protein-ligand association states. Anal. Biochem. *299*, 136–146.

29. Wyatt Tech Note TN1006, Performing a Protein Conjugate Analysis in ASTRA and References Therein.

30. Wyatt Tech Note TN4002, The Refractive Index Increment of Proteins

31. Theisen, A., Johann, C., Deacon, M.P., and Harding, S.E. (2000). Refractive Increment Data-Book (Nottingham University Press).

32. Nieuwenhuysen, P., De Voeght, F., and Clauwaert, J. (1981). The molecular weight of Artemia ribosomes, as determined from their refractive-index increment and light-scattering intensity. Biochem. J. *197*, 689–693.